2008

Kinetic Evaluation of Highly Active Supported Gold Catalysts Prepared from Monolayer-Protected Clusters: An Experimental Michaelis-Menten Approach for Determining the Oxygen Binding Constant during CO Oxidation Catalysis

Cormac G. Long
Trinity University

John D. Gilbertson
Trinity University

G. Vijayaraghavan

K. J. Stevenson

Christopher J. Pursell
Trinity University, cpursell@trinity.edu

See next page for additional authors

J|A|C|S
ARTICLES

Published on Web 07/12/2008

Kinetic Evaluation of Highly Active Supported Gold Catalysts Prepared from Monolayer-Protected Clusters: An Experimental Michaelis−Menten Approach for Determining the Oxygen Binding Constant during CO Oxidation Catalysis

Cormac G. Long,[†] John D. Gilbertson,[†] Ganesh Vijayaraghavan,[‡] Keith J. Stevenson,[‡] Christopher J. Pursell,[†] and Bert D. Chandler*[,†]

Departments of Chemistry, Trinity University, San Antonio, Texas 78212-7200, and University of Texas at Austin, 1 University Station A5300, Austin, Texas 78712-0165

Received February 25, 2008; E-mail: bert.chandler@trinity.edu

Abstract: Thiol monolayer-protected Au clusters (MPCs) were prepared using dendrimer templates, deposited onto a high-surface-area titania, and then the thiol stabilizers were removed under H_2/N_2. The resulting Au catalysts were characterized with transmission electron microscopy, X-ray photoelectron spectroscopy, and infrared spectroscopy of adsorbed CO. The Au catalysts prepared via this route displayed minimal particle agglomeration during the deposition and activation steps. Structural data obtained from the physical characterization of the Au catalysts were comparable to features exhibited from a traditionally prepared standard Au catalyst obtained from the World Gold Council (WGC). A differential kinetic study of CO oxidation catalysis by the MPC-prepared Au and the standard WGC catalyst showed that these two catalyst systems have essentially the same reaction order and Arrhenius apparent activation energies (28 kJ/mol). However, the MPC-prepared Au catalyst shows 50% greater activity for CO oxidation. Using a Michaelis−Menten approach, the oxygen binding constants for the two catalyst systems were determined and found to be essentially the same within experimental error. To our knowledge, this kinetic evaluation is the first experimental determination of oxygen binding by supported Au nanoparticle catalysts under working conditions. The values for the oxygen binding equilibrium constant obtained from the Michaelis−Menten treatment (ca. 29−39) are consistent with ultra-high-vacuum measurements on model catalyst systems and support density functional theory calculations for oxygen binding at corner or edge atoms on Au nanoparticles and clusters.

Introduction

As a noble metal typically coordinated by soft ligands such as phosphines, gold has a low affinity for oxygen. Silver and copper, the other group IB homologues, possess extended oxide chemistries, yet only a small number of metastable gold−oxygen compounds are known. This low affinity for oxygen extends to both bulk and nanoparticulate gold and is largely responsible for gold's remarkable ability to catalyze oxidation reactions.[1] In particular, high CO oxidation activity of supported gold catalysts at sub-ambient temperatures has been well documented over the past 20 years.[1,2] More recent studies of gold and gold-based heterogeneous catalysts have extended the number of gold-catalyzed reactions to important reactions for industrial and synthetic chemists, including the water−gas shift reaction,[3] alcohol[4] and alkene[5] oxidations, hydrosilation,[6,7] the selective hydrogenation of nitroaromatics,[8,9] and the production of commodity chemicals from biological feedstocks.[10]

In spite of the tremendous research activity in gold-catalyzed oxidation reactions, the origins of the catalytic activity are not well understood. Indeed, oxygen binding and activation, the importance of the support in affecting catalytic activity, the Au oxidation state necessary for high activity, the sensitivity to water, and the strong dependence on particle size and morphology are all examples of currently unresolved issues.[2] Computational studies are beginning to address some of these problems; however, different models suggest a variety of answers to the key issues.[11] Studies on model systems under ultra-high-vacuum

[†] Trinity University.
[‡] University of Texas at Austin.

(1) Bond, G. C.; Louis, C.; Thompson, D. T. *Catalysis by Gold*; Imperial College Press: London, 2006; Vol. 6.
(2) Kung, M. C.; Davis, R. J.; Kung, H. H. *J. Phys. Chem. C* **2007**, *111*, 11767–11775.
(3) Fu, Q.; Saltsburg, H.; Flytzani-Stephanopoulos, M. *Science (Washington, DC)* **2003**, *301*, 935–938.
(4) Enache, D. I.; Edwards, J. K.; Landon, P.; Solsona-Espriu, B.; Carley, A. F.; Herzing, A. A.; Watanabe, M.; Kiely, C. J.; Knight, D. W.; Hutchings, G. J. *Science (Washington, DC)* **2006**, *311*, 362–365.
(5) Hughes, M. D.; Xu, Y.-J.; Jenkins, P.; McMorn, P.; Landon, P.; Enache, D. I.; Carley, A. F.; Attard, G. A.; Hutchings, G. J.; King, F.; Stitt, E. H.; Johnston, P.; Griffin, K.; Kiely, C. J. *Nature (London, UK)* **2005**, *437*, 1132–1135.
(6) Corma, A.; Gonzalez-Arellano, C.; Iglesias, M.; Sanchez, F. *Angew. Chem., Int. Ed.* **2007**, *46*, 7820–7822.
(7) Corma, A.; Serna, P. *Science (Washington, DC)* **2006**, *313*, 332–334.
(8) Boronat, M.; Concepcion, P.; Corma, A.; Gonzalez, S.; Illas, F.; Serna, P. *J. Am. Chem. Soc.* **2007**, *129*, 16230–16237.
(9) Corma, A.; Concepcion, P.; Serna, P. *Angew. Chem., Int. Ed.* **2007**, *46*, 7266–7269.
(10) Christensen, C. H.; Joergensen, B.; Rass-Hansen, J.; Egeblad, K.; Madsen, R.; Klitgaard, S. K.; Hansen, S. M.; Hansen, M. R.; Andersen, H. C.; Riisager, A. *Angew. Chem., Int. Ed.* **2006**, *45*, 4648–4651.

(UHV) conditions have also shed considerable light onto the unique activity of Au catalysts.[12–14] Unfortunately, these studies of well-defined model catalysts are limited by the well-known pressure and materials gaps. Further, a recent review highlights the difficulties of preparing active supported nanoparticle catalysts and the challenges of comparing them to model systems.[2] Even small amounts of impurities (particularly chloride) act as severe poisons for CO oxidation and make it difficult to evaluate catalysts prepared via various means and analyzed in different laboratories.

Consequently, it is essential to develop new, functional models of Au catalysts in order to elucidate their structure−property relationships. A functional model catalyst should have a known and reproducible synthetic history and, critically, have structures and catalytic activity comparable to those of the most active systems. The precise synthesis of catalysts would provide opportunities to controllably adjust catalyst parameters to evaluate reaction mechanisms and to assess structure−property−activity trends. Effective models would allow the catalyst community to probe support effects, understand the influence of introducing additional metals into the system, and possibly begin to bridge the pressure and materials gaps.

The variety of emerging solution-based nanoparticle syntheses being developed around the world offer new promise for preparing model supported catalysts. Because the synthetic methods are often well understood, the resulting catalysts have reproducible synthetic histories. In general, most synthetic schemes use ligand or polymer stabilizers to prepare colloidal nanoparticles. The nanoparticles are then deposited onto a support (a high-surface-area oxide or single crystal substrate), and the stabilizing organic material is thermally removed to activate the catalyst. Several research groups used this approach, employing dendrimer encapsulated nanoparticles,[15–18] monolayer-protected clusters,[19–25] and polymer-stabilized colloids[26,27] as catalyst precursors.

For supported gold catalysts, the issue of removing the nanoparticle stabilizers is critical, as catalytic activities can be dramatically diminished by residual stabilizer impurities, which can act as poisons. A few studies have used dendrimer-encapsulated nanoparticles[17,28,29] or thiol monolayer-protected clusters (MPCs)[19–25] to prepare Au catalysts for several reactions. Although catalytic activities are generally reported, most of these studies do not *quantitatively* compare their catalysts to those reported in the literature. This comparison is critical if these synthetic schemes are going to shed light on "real-world catalysts" and make meaningful contributions to understanding the most active sites for a given catalytic reaction.

The significance of this work is two-fold, as the following study undertakes two primary tasks. First, we prepared supported gold catalysts from Au MPCs and show that this is a viable means of preparing functional model catalysts with activities and physical properties comparable to those of traditionally prepared catalysts. This presents a number of new opportunities for studying gold catalysts, because the MPCs are prepared separately from the support. This will allow for a more systematic evaluation of factors such as support effects and chloride poisoning on catalytic activity, both of which are important parameters for gold catalysis.

Second, we applied a Michaelis−Menten kinetic treatment to characterize and describe these catalysts. This treatment provides a fresh examination of gold-catalyzed CO oxidation, yielding quantitative measures of the similarities and differences between catalysts prepared by entirely different methods. The Michaelis−Menten treatment also provides important information regarding the catalyst active site that has not been previously reported. To our knowledge, the kinetic treatment described below provides the first experimental measurement of an O_2 binding constant for Au catalysts and also allows us to compare the relative number of active sites on two catalysts. These critical catalyst parameters offer new opportunities to evaluate computational and UHV models for Au catalysts, which may shed some light on the nature of the catalytic active site. Future applications of the Michaelis−Menten model will also allow for quantitative evaluations of catalytic activity with changes in catalyst properties (e.g., support, promoter/inhibitor addition). Thus, the combination of the MPC catalyst preparation and the Michaelis−Menten kinetic treatment opens the door to studies on the nature and number of active sites that previously have not been possible.

Experimental Section

Materials and Reagents. Hydroxyl-terminated, generation 5 polyamidoamine (PAMAM) dendrimers (G5OH) were purchased as a 5% methanolic solution from Dendritech. Prior to use, methanol was removed by rotary evaporation at room temperature. $HAuCl_4$ (Alfa), decanethiol (Aldrich), and $NaBH_4$ (Aldrich) were used as received. Reagent-grade toluene, methylene chloride, hexanes, and ethanol were dried over molecular sieves (Davison, grade 564, 3 Å) and otherwise used as received. Water was purified to a resistivity of 17−18 MΩ-cm with a Barnstead Nanopure system. P25 Titania (Aerolyst 7711) was generously provided by Degussa Corp. The World Gold Council test catalyst was purchased from the World Gold Council.

Characterization. Solution UV−visible absorbance spectra were collected on a Jasco V-530 spectrometer using quartz cells.

(11) Janssens, T. V. W.; Clausen, B. S.; Hvolbaek, B.; Falsig, H.; Christensen, C. H.; Bligaard, T.; Norskov, J. K. *Top. Catal.* **2007**, *44*, 15–26.
(12) Chen, M. S.; Goodman, D. W. *Science (Washington, DC)* **2004**, *306*, 252–255.
(13) Stiehl, J. D.; Kim, T. S.; McClure, S. M.; Mullins, C. B. *J. Am. Chem. Soc.* **2004**, *126*, 13574–13575.
(14) Matthey, D.; Wang, J. G.; Wendt, S.; Matthiesen, J.; Schaub, R.; Laegsgaard, E.; Hammer, B.; Besenbacher, F. *Science (Washington, DC)* **2007**, *315*, 1692–1696.
(15) Lafaye, G.; Siani, A.; Marecot, P.; Amiridis, M. D.; Williams, C. T. *J. Phys. Chem. B* **2006**, *110*, 7725–7731.
(16) Lang, H.; May, R. A.; Iversen, B. L.; Chandler, B. D. *J. Am. Chem. Soc.* **2003**, *125*, 14832–14836.
(17) Lang, H.; Maldonado, S.; Stevenson, K. J.; Chandler, B. D. *J. Am. Chem. Soc.* **2004**, *126*, 12949–12956.
(18) Scott, R. W. J.; Sivadinarayana, C.; Wilson, O. M.; Yan, Z.; Goodman, D. W.; Crooks, R. M. *J. Am. Chem. Soc.* **2005**, *127*, 1380–1381.
(19) Zheng, N.; Stucky, G. D. *J. Am. Chem. Soc.* **2006**, *128*, 14278–14280.
(20) Pietron, J. J.; Stroud, R. M.; Rolison, D. R. *Nano Lett.* **2002**, *2*, 545–549.
(21) Chou, J.; McFarland, E. W. *Chem. Commun.* **2004**, 1648–1649.
(22) Chou, J.; Franklin, N. R.; Baeck, S.-H.; Jaramillo, T. F.; McFarland, E. W. *Catal. Lett.* **2004**, *95*, 107–111.
(23) Hickey, N.; Larochette, P. A.; Gentilini, C.; Sordelli, L.; Olivi, L.; Polizzi, S.; Montini, T.; Fornasiero, P.; Pasquato, L.; Graziani, M. *Chem. Mater.* **2007**, *19*, 650–651.
(24) Konya, Z.; Puntes, V. F.; Kiricsi, I.; Zhu, J.; Ager, J. W., III; Ko, M. K.; Frei, H.; Alivisatos, P.; Somorjai, G. A. *Chem. Mater.* **2003**, *15*, 1242–1248.
(25) Budroni, G.; Corma, A. *Angew. Chem., Int. Ed.* **2006**, *45*, 3328–3331.
(26) Yang, M.; Rioux, R. M.; Somorjai, G. A. *J. Catal.* **2006**, *237*, 255–266.
(27) Bratlie, K. M.; Lee, H.; Komvopoulos, K.; Yang, P.; Somorjai, G. A. *Nano Lett.* **2007**, *7*, 3097–3101.
(28) Korkosz, R. J.; Gilbertson, J. D.; Prasifka, K. S.; Chandler, B. D. *Catal. Today* **2007**, *122*, 370–377.
(29) Auten, B.; Crump, C. J.; Singh, A. R.; Chandler, B. D. In *Catalysis of Organic Reactions*; Schmidt, S. R., Ed.; CRC Press: Boca Raton, FL, 2006; pp 315−323..

Transmission electron microscopy (TEM) analysis of the nanoparticles was performed with a JEOL 2010F instrument operating at 200 kV. Au nanoparticles suspended in hexane were drop-cast onto a 150 mesh Cu TEM grid covered with a thin amorphous carbon film. Supported Au nanoparticles were suspended in ethanol prior to drop-casting. Image analysis was performed with DigitalMicrograph 3.6.1 (Gatan) software. Elemental analyses were performed by Desert Analytics (Tucson, AZ). DRIFT spectra were collected on a Thermo-Nicolet Nexus 470 FT-IR spectrometer using a Thermo-Electron environmental cell accessory. Atomic absorption spectroscopy was performed on a Varian Spectra AA 220 FS spectrometer, using sample preparations reported previously.[30] Briefly, the samples were digested in fresh aqua regia at 60 °C for 3 h. The solution was filtered and the pH adjusted to 4−6 before the samples were analyzed. MPC samples were treated in a vacuum oven at 80 °C overnight before being dissolved in aqua regia.

DEN Synthesis. Aqueous solutions of Au dendrimer-encapsulated nanoparticles (Au-DENs) were prepared according to literature procedures.[31] Briefly, an aqueous solution of G5OH (50 mL, 5.5 μM) was mixed with an aqueous solution of $HAuCl_4$ (2 mL, 20 mM, 147:1 Au:G5OH molar ratio). After this mixture was stirred for 3 min, excess $NaBH_4$ in 0.1 M NaOH was added to the yellow solution, instantly producing the characteristic brown solution of G5OH(Au_{147}) DENs.

MPC Extraction and Deposition. Nanoparticle extraction was performed according to the literature procedure.[31] Briefly, after the DEN solution was stirred for 1 h, 100 equiv of solid $NaBH_4$ was added. The solution was then extracted with an equal volume of toluene containing 125 mol of excess of decanethiol by shaking in a separatory funnel for 5 min. The Au MPCs in the toluene layer were separated and concentrated to ca. 3 mL by rotary evaporation. The solution was then purified by placing 1 mL into a centrifuge tube and precipitating with 15 mL of ethanol, followed by centrifugation for 20 min. After the supernatant was decanted, the Au MPCs were redissolved into hexanes, precipitated, and centrifuged a second time, followed by redissolution into either hexanes or methylene chloride.

The purified Au MPCs were deposited onto TiO_2 by adapting a literature method.[19] Briefly, sufficient Au MPCs to produce a 0.2 wt % Au loading were dissolved in a minimum amount of methylene chloride and added to a vigorously stirring suspension of 100 mg of TiO_2 in 5 mL of methylene chloride. The suspension was stirred until the methylene chloride was no longer colored (ca. 5 min). The TiO_2 was then rinsed threee times with 5 mL of methylene chloride and dried in air for 1 h at 393 K. Higher Au loadings (2.4 wt %) were achieved by adjusting the Au MPC/TiO_2 ratio.

Thiol Removal. The Au MPC-loaded TiO_2 samples (typically 100 mg) were placed in a tube furnace and treated under flowing H_2/N_2 (50/50 mixture, 20 mL/min) at 563 K for 16 h. The initial ramp in temperature from 298 to 563 K was 2.2 K/min for 2 h.

X-ray Photoelectron Spectroscopy (XPS). X-ray photoelectron spectra were collected using a Kratos AXIS Ultra DLD photoelectron spectrophotometer using a monochromatic aluminum X-ray source at 160 W. Each analysis started with a survey scan from 0 to 1200 eV with a dwell time of 100 ms and a pass energy of 160 eV at steps of 1 eV with one sweep. For the high-resolution analysis, the number of sweeps was increased, the pass energy was lowered to 60 eV at steps of 100 meV, and the dwell time was changed to 1000 ms. To exclude any effects on the values of binding energies due to charging of the sample during the XPS analysis, all data were corrected using the AXIS charge-neutralization system, which provides charge compensation on all types of conductive materials and is particularly important when using a monochromatic X-ray source.

Infrared Spectroscopy of Adsorbed CO. Fourier transform infrared (FT-IR) spectra were collected using a Thermo-Nicolet Nexus 470 spectrometer equipped with a DTGS detector with a resolution of 16 cm^{-1}. A powder sample was placed in an *in situ* DRIFT cell (Thermo-SpectraTech), sealed, and treated under flowing H_2 at 423 K for 30 min. The cell was flushed with He at 423 K for 30 min and cooled to 293 K under flowing He (5 min), and then a background spectrum of the sample was collected (32 scans). Flowing CO (5% in He) was then introduced to the sample chamber for 5 min, and a spectrum was recorded. Reference spectra of gas-phase CO and CO_2 were subtracted from sample spectra using the Omnic software, yielding the spectrum of CO adsorbed on the catalyst.

CO Oxidation Catalysis. The CO oxidation reactor system (schematic in Supporting Information) consisted of a custom-built laboratory-scale single-pass plug−flow microreactor (39 mm in length, with an internal diameter of 7 mm). CO, O_2, and N_2 feed gases were UHP grade contained in aluminum cylinders (Matheson-Trigas). Gas flows were regulated using Porter Instruments series 100 mass flowmeters and controlled by a PCIM4 computer interface module (Porter Instrument Co. Inc.). Individual gas flows were adjusted such that a constant volumetric flow of 27 mL/min was maintained in all experiments. Gases passed through a mixing chamber positioned immediately after the mass flow controllers. CO, O_2, and N_2 concentrations were determined with an online downstream IR adsorption gas analyzer (Siemens Ultramat 23). Catalyst heating was achieved with a temperature-controlled tube furnace (Thermolyne model 21100). For kinetics measurements, the tube furnace was removed and replaced with an ethylene glycol bath, cooled by a Thermo-Haake EK 45 cooling system. Catalyst temperature was monitored using a thermocouple embedded in the catalyst and a process control monitor (Omega Engineering).

Supported catalyst samples were diluted 1250:1 with 400-mesh silicon carbide (Aldrich) and placed in the microreactor. The diluted catalyst mass, nominally 250 mg, was adjusted to maintain differential reactor conditions, and the conversions studied were always between 1 and 2%. Catalysts were pretreated *in situ* by heating to 523 K under flowing nitrogen, followed by a 30 min $H_2/O_2/N_2$ 25/25/50 treatment. All catalysts studied showed stable activity (minimal change in conversion) for several hours after this pretreatment. Changes in CO oxidation activity were measured as a function of temperature as well as CO (0.2−1%) and O_2 (5−20%) concentration. All activities were determined by averaging steady-state conversion data for approximately 2 h, usually between 1 and 3 h after introducing CO to the activated catalyst. Each activity measurement was performed with a fresh catalyst sample.

Results and Discussion

Synthesis of Supported Gold Catalysts. Several synthetic methods are available for the preparation of Au MPCs, with the Brust−Schiffrin method being the most common.[32,33] Although slightly more demanding from a synthetic standpoint, the dendrimer templating method has the advantage of exerting substantial control over particle size, composition, and morphology relative to standard MPC syntheses.[34,35] Given our experience with dendrimer-mediated syntheses,[16,17,36] we prepared the supported gold catalysts using MPCs extracted from DENs, as described previously (see Experimental Section for details).[28,31]

(30) Lang, H. M., R. A.; Iversen, B. L.; Chandler, B. D. *J. Am. Chem. Soc.* **2003**, *125*, 14832–14836.
(31) Garcia-Martinez, J. C.; Crooks, R. M. *J. Am. Chem. Soc.* **2004**, *126*, 16170–16178.
(32) Brust, M.; Kiely, C. J. *Colloids Surf. A: Physicochem. Eng. Aspects* **2002**, *202*, 175–186.
(33) Brust, M.; Walker, M.; Bethell, D.; Schiffrin, D. J.; Whyman, R. *J. Chem. Soc., Chem. Commun.* **1994**, 801–802.
(34) Scott, R. W. J.; Wilson, O. M.; Crooks, R. M. *J. Phys. Chem. B* **2005**, *109*, 692–704.
(35) Chandler, B. D.; Gilbertson, J. D. In *Dendrimer Catalysis*; Gade, L., Ed.; Topics in Organometallic Chemistry *21*; Springer: Berlin, 2006; pp 97−120..
(36) Gilbertson, J. G.; Vijayaraghavan, G.; Stevenson, K. J.; Chandler, B. D. *Langmuir* **2007**, *23*, 11239–11245.

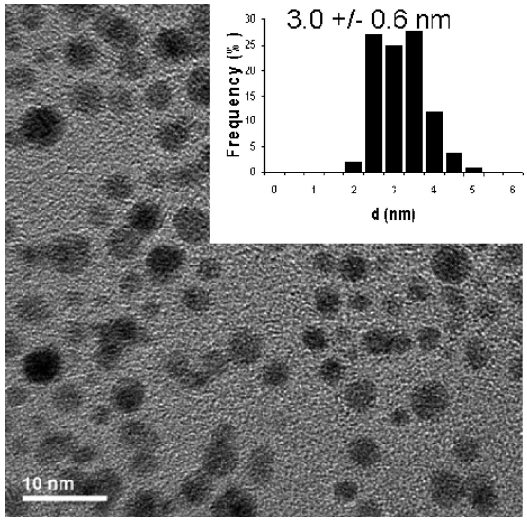

Figure 1. TEM micrograph of Au MPCs. The inset is the particle size distribution histogram (100 particles).

UV−visible spectra for the original DENs and the MPCs were consistent with published spectra and are available as Supporting Information. A representative TEM micrograph and particle size distribution for the $C_{10}S$(Au) MPCs in Figure 1 shows the MPCs to be 3.0 ± 0.6 nm in diameter and fairly monodisperse. The activity of supported gold catalysts strongly depends on particle size,[37,38] and several groups have reported a maximum in activity with particles ~3 nm in diameter.[1] Consequently, the MPC preparation method is well suited to preparing nanoparticles comparable to those found in the most active supported gold catalysts.[1]

MPC Deposition and Thiol Removal. The Au MPCs capped with decanethiol ($C_{10}S$) were deposited onto Degussa P25 TiO_2[39] by stirring the brown MPCs solution with the oxide support, similar to the method reported by Stucky and co-workers.[19] After contacting the titania, the solution rapidly lost color and the oxide picked up a gray/purple tint, indicating the spontaneous adsorption of the Au MPCs onto the support. TEM analysis of the gray support after drying in air at 393 K for 1 h shows electron-rich regions that are attributable to Au MPCs on the less-electron-dense oxide. Figure 2a shows that the average particle size of the supported MPCs was found to be 2.8 ± 0.8 nm; thus, no particle growth was observed during deposition of the MPCs onto the oxide.

Figure 2b shows that the average particle size of the supported Au nanoparticles is 3.4 ± 0.8 nm after treatment at 563 K for 16 h under flowing H_2/N_2 (50/50) to remove capping thiol ligands. This treatment was chosen on the basis of our previous work with supported MPCs and is consistent with previous thermogravimetric analysis (TGA) data on thiol desorption from MPCs.[28,40] The activated nanoparticles (3.4 ± 0.8 nm) are slightly larger than the deposited Au MPCs (2.8 ± 0.8 nm), which suggests a small degree of agglomeration during thiol removal. Even with the small increase in particle size, the resulting catalysts are well within the particle size range expected for active Au/TiO_2 catalysts, and the average particle size is within the standard deviation of the distribution determined for the WGC test catalyst (*vide infra*).[1] Bulk elemental analysis and XPS (*vide infra*) of the activated NPs showed the sulfur content to be below the detection limit (<0.01%). Importantly, shorter treatment times (e.g., 4 h at 563 K) led to inactive catalysts and to yellowing of the reactor tubes during CO oxidation experiments, presumably due to residual sulfur on the nanoparticles (*vide infra*).

Activation of WGC Catalyst. A critical component of a functional model catalyst is that the material should have catalytic activity comparable to that of recognized standards. For supported gold catalysts, a reference Au/TiO_2 catalyst, prepared in Haruta and Tsubota's laboratories, was obtained from the World Gold Council.[41] This material consists of 1% Au supported on Degussa P25 TiO_2 and is hereafter referred to as the WGC catalyst. It is among the most active CO oxidation catalysts. To properly compare the catalytic activity of the two materials, the WGC catalyst was subjected to the same treatment as the Au MPC catalyst.[42] Figure 3 shows the average Au particle size of the untreated standard catalyst to be 3.2 ± 1.0 nm. After treatment of the WGC catalyst under flowing H_2/N_2 (50/50) for 16 h at 563 K, the average particle size remains unchanged (3.2 ± 0.7 nm). These values are also comparable to the size of the MPC catalyst before and after the same treatment (3.4 ± 0.8 nm).

Infrared spectroscopic studies were also used to probe the Au MPC and standard WGC catalysts. Each sample was subjected to a brief *in situ* pretreatment at 423 K to clean and dry the surface prior to introducing CO to the catalyst. DRIFT-IR spectra under flowing CO (Figure 4) of the two samples are nearly identical (ν_{CO} = 2115 and 2111 cm^{-1}). The small difference in the ν_{CO} values for the MPC and WGC catalysts is primarily due to the data spacing from the resolution, which is required to accurately subtract the gas-phase CO and CO adsorbed on titania. The ν_{CO} values obtained for these catalyst are in good agreement with other reported values for active Au catalysts and are consistent with the ν_{CO} of Au^0 on TiO_2.[1]

Both catalysts were evaluated with XPS, and survey scans can be found as Supporting Information. We see no evidence of a sulfur 2p peak (usually found at 164 eV) in the XPS spectrum of the treated Au MPC catalyst, indicating that the vast majority of the sulfur is removed from the catalyst by the long-term reduction in H_2/N_2. High-resolution XPS studies are shown in Figure 5. For both the Au MPC and WGC catalysts, the Au 4f peaks showed identical binding energies of 80.5 and 84.1 eV. Thus, the XPS results are consistent with the IR and TEM data, indicating that the primary properties of the WGC and Au MPC catalysts are indistinguishable after the reduction treatment used to remove the alkyl thiols. The XPS and IR data cannot completely rule out the possibility that small amounts of sulfur may remain on the catalyst; however, if trace amounts of sulfur remain, they do not have measurable effects on the physical properties of the catalyst.

The extended reducing treatment (H_2/N_2 at 300 °C for 16 h) is necessary to remove capping alkyl thiols from the deposited MPCs in order to prepare active catalysts. Supported MPCs treated under these conditions for times as long as 8 h were

(37) Valden, M.; Lai, X.; Goodman, D. W. *Science* **1998**, *281*, 5383.
(38) Chen, M. S.; Goodman, D. W. *Science* **2004**, *306*, 252–255.
(39) P25 TiO_2 is a commercial mixture of rutile and anatase that is widely used as a support for active Au catalysts.
(40) Isaacs, S. R.; Choo, H.; Ko, W.-B.; Shon, Y.-S. *Chem. Mater.* **2006**, *18*, 107–114.
(41) The World Gold Council catalyst is prepared via deposition−precipitation of auric acid onto titania, drying, and calcination at 673 K for 1 h.
(42) The activity of the WGC catalyst after the reduction treatment was comparable to its activity after the standard oxidation protocol suggested by the catalyst manufacturers.

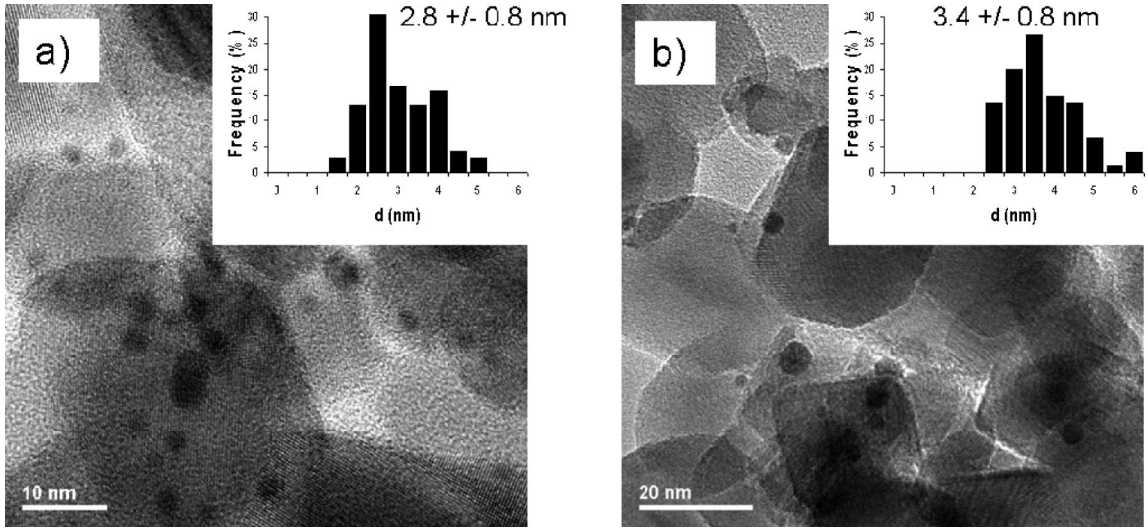

Figure 2. TEM micrographs of $C_{10}S$(Au) MPCs deposited on TiO_2 (a) before and (b) after treatment at 563 K for 16 h under flowing H_2/N_2 (50/50). The inset of each TEM micrograph is the corresponding particle size distribution histogram (139 particles for panel a, and 75 particles for panel b). Note that the scale bars are different for the two micrographs.

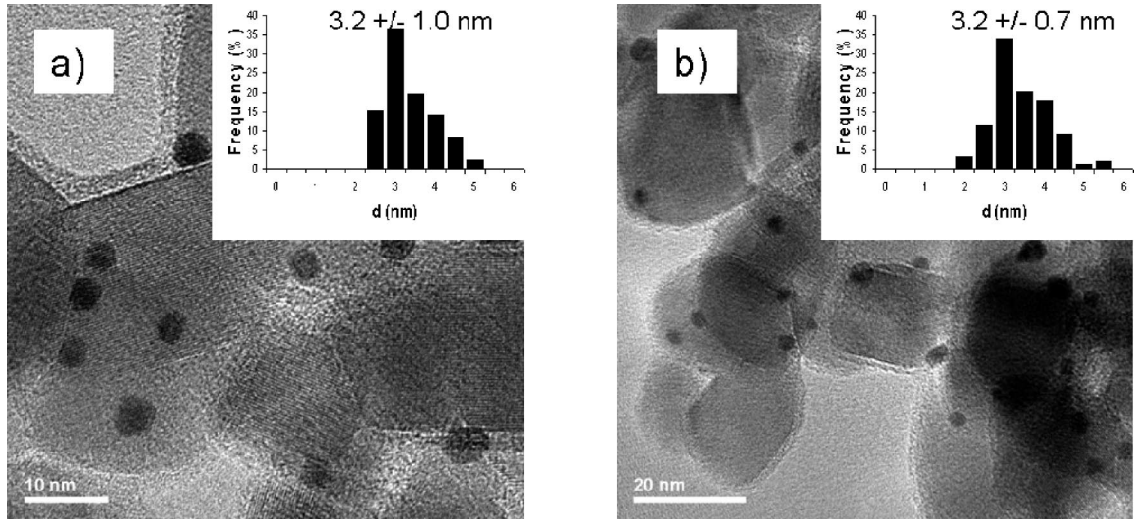

Figure 3. TEM micrographs of the standard WGC catalyst (a) before and (b) after treatment at 563 K for 16 h under flowing H_2/N_2 (50/50). The inset of each TEM micrograph is the corresponding particle size distribution histogram (71 particles for panel a, and 88 particles for panel b). Note that the scale bars are different for the two micrographs.

inactive for CO oxidation, thus necessitating such a long treatment. Although this is a potentially pro-sintering treatment, only limited agglomeration was observed for the MPC catalyst, and the WGC catalyst showed no visible signs of sintering at all. Considering the nature of the pretreatment employed and the reducibility of the support, it may be possible that vacancies or surface defects are created on the support during the pretreatment; these sites might play a role in preventing particle agglomeration. Chen and Goodman suggest that defects on oxide supports play a role in limiting the nucleation and growth of metal nanoparticles as well as in defining their electronic properties.[43] Several reports have also demonstrated that Au particles bind more strongly to a defect-rich surface relative to a defect-deficient surface.[44–46]

Given this potential for sintering, it is important to consider the possibility that the extended reduction may fundamentally change the catalyst. As a control for this, we examined the catalytic activity of the WGC catalyst with and without the 16 h reduction treatment required to activate the MPC catalyst (plot in Supporting Information). We found essentially the same catalytic activity before and after the reduction treatment, although the untreated sample showed slightly greater deactivation relative to the treated WGC and MPC catalysts. Even if Ti^{III} sites are produced during the treatment, they would be expected to quickly react with O_2 under CO oxidation conditions. Additionally, the catalytic activity of both the WGC and MPC catalysts is in good agreement with the most active catalysts reported in the literature, which have not undergone extended reduction treatments.[2] So, although we cannot rule out the possibility that the thiol removal treatment may cause a small degree of titania reduction, it does not appear to induce sufficient changes to the catalyst to differentiate the catalysts reported here from those reported in the literature.

(43) Chen, M.; Goodman, D. W. *Acc. Chem. Res.* **2006**, *39*, 739–746.
(44) Chen, M. S.; Goodman, G. W. *Science* **2004**, 306.
(45) Lopez, N.; Norskov, J. K.; Janssens, T. V. W.; Carlson, A.; Puig-Mullina, A.; Clausen, B. S.; Grunwaldt, J. D. *J. Catal.* **2004**, *225*, 84.
(46) Valden, M.; Lai, X.; Goodman, D. W. *Science* **1998**, *281*, 1647.

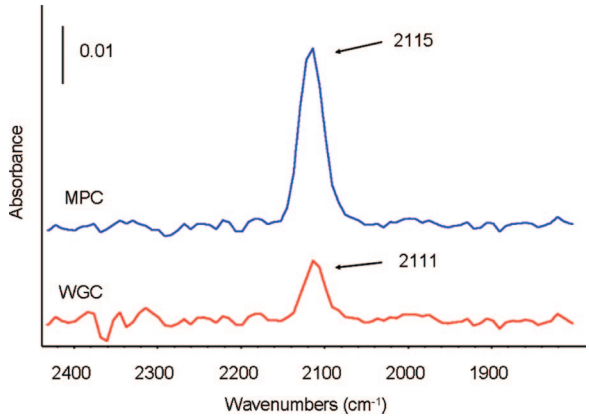

Figure 4. DRIFT spectra of the Au MPC (2.4 wt % Au) and WGC (1 wt % Au) catalysts at 293 K under flowing CO (5% in He) at 16 cm^{-1} resolution. The catalysts were pretreated at 423 K in flowing H_2 for 30 min and at 423 K in flowing He for 30 min prior to introduction of the CO. CO absorbed on TiO_2 as well as gas-phase CO and CO_2 were subtracted from the spectra.

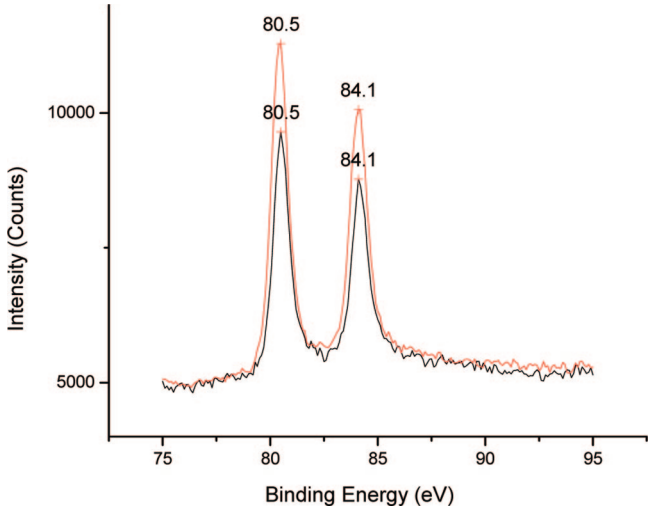

Figure 5. High-resolution XPS scan of the Au 4f peaks from the MPC (bottom, black) and WGC (top, red) catalysts after treatment in H_2/N_2 for 16 h.

Catalyst Activity Measurements. Although numerous studies have investigated CO oxidation by supported Au catalysts, there are few detailed kinetic studies of these materials under differential reactor conditions, where intrinsic rates are more appropriately studied. Careful studies under UHV conditions suffer from the pressure and materials gaps and therefore are not easily compatible with flow experiments to evaluate catalytic turnovers. With the notable exception of an isotopic transient analysis study by Calla and Davis,[47–49] most CO oxidation catalysts have been studied with light-off curves, where temperature is ramped and conversions approach 100%. Although light-off curves are an effective means of evaluating and comparing catalysts, the exothermic nature of CO oxidation can yield artificially high conversions. Thus, most light-off curve experiments are not suitable for examining intrinsic reaction rates.

In the present study, the mass of the catalyst was adjusted to maintain differential reaction conditions, and conversions were always between 1 and 2%. Figure 6 shows a plot of CO oxidation activity at 293 K versus time for the MPC and WGC catalysts. Catalyst activity typically showed a slight decrease in activity in the first hour on-stream, after a brief pretreatment designed to remove adsorbates from the catalyst surface. After this initial drop in activity, the catalysts were stable for several hours. Catalytic activities at a particular temperature, CO pressure, and O_2 pressure were determined from the average of the rate measurements collected after the catalyst had reached steady-state conditions, typically for 2 h on-stream. Under these conditions, the MPC catalyst showed activities roughly 50% higher than those of the WGC catalyst.

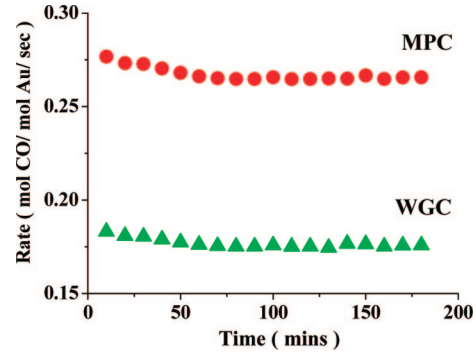

Figure 6. Change in catalytic activity over time for the WGC and MPC catalysts. Steady-state activity measurements were determined only after the rate stabilized (ca. 1 h).

Reaction orders for CO and O_2 were determined for both catalysts in the steady-state regime. Both catalysts showed zero-order dependence on CO content between 0.2 and 1.0% CO with 20% O_2 in the feed (figure available as Supporting Information). The zero-order CO dependence indicates only that the catalyst is kinetically saturated; it does not require the entire catalyst surface to be physically saturated (i.e., every surface atom bound to a CO molecule) under reaction conditions ($\leq$8 Torr). Previous IR spectroscopy studies of CO adsorption show that supported Au catalysts bind additional CO as pressures increase to 150 Torr, or roughly 20−100 times the CO pressure used in this study.[50] This indicates that surface Au sites are indeed available under reaction conditions and that the catalysts are only kinetically saturated.

Oxygen dependence plots, determined at pressures ranging from 5 to 20% O_2, were studied to characterize the active site under real working conditions at 268, 273, 283, and 293 K with 1% CO and are shown in Figure 7. The oxygen reaction order was extremely consistent for both catalysts in the temperature range studied, varying between 0.18 and 0.20 (values are available as Supporting Information). Both the CO and O_2 reaction orders are consistent with light-off curve measurements for CO oxidation over supported Au catalysts.[1]

Arrhenius plots for both catalysts using 20% O_2 and 1% CO in the feed were prepared and are shown in Figure 8. Each data set shows a strong linear correlation, and the extracted apparent activation energies of ca. 28 kJ/mol are the same within the experimental error of the measurements. Activation energies determined at lower O_2 pressures were also within the measurement errors. These values are comparable to most activation energies reported for CO oxidation over supported gold catalysts (~30 kJ/mol).[1]

(47) Calla, J. T.; Davis, R. J. *J. Catal.* **2006**, *241*, 407–416.
(48) Calla, J. T.; Davis, R. J. *Ind. Eng. Chem. Res.* **2005**, *44*, 5403–5410.
(49) Calla, J. T.; Davis, R. J. *J. Phys. Chem. B* **2005**, *109*, 2307–2314.
(50) Derrouiche, S.; Gravejat, P.; Bianchi, D. *J. Am. Chem. Soc.* **2004**, *126*, 13010–13015.

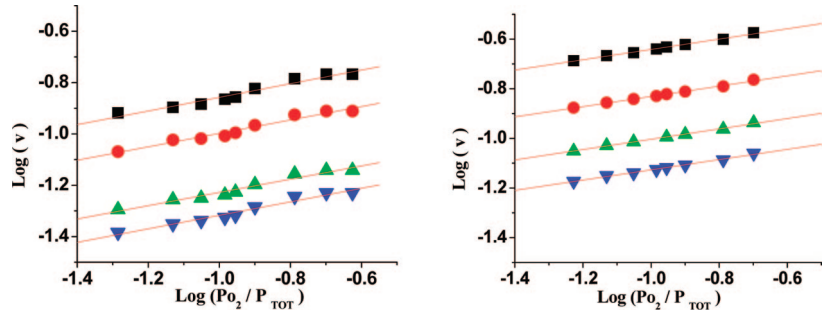

Figure 7. Oxygen reaction order plots for the WGC (left) and MPC (right) catalysts at (top to bottom) 293, 283, 273, and 268 K.

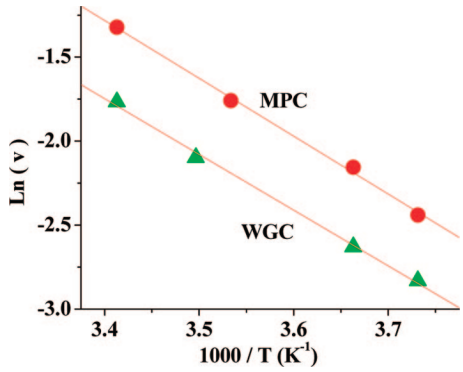

Figure 8. Arrhenius plots of MPC and WGC catalysts. Apparent activation energies determined from the plots are 28.6 ± 1.0 and 27.6 ± 1.0 kJ/mol for the MPC and WGC catalysts, respectively.

In order for MPC catalysts to serve as functional models for traditionally prepared Au catalysts, they must have catalytic activity comparable to that of systems of interest, namely the highly active low-temperature CO oxidation catalysts. The CO oxidation activities of the WGC and MPC catalysts are entirely consistent with literature data for the most active Au catalysts and are higher than many reported in the literature.[2] At 273 K, the Haruta,[51] Davis,[47,49] Schüth,[52] and van Bokhoven[53] groups have reported catalyst activities between 0.1 and 0.3 mol $CO \cdot mol^{-1}$ $Au \cdot s^{-1}$, and both of the catalysts in the present study have activities in this range. Lower reported activities, which are common, have been suggested to be due to poisoning by trace amounts of chloride remaining from the preparation.[2] The similarity in the activities found for the MPC catalyst and those reported by other groups provides further confidence that very few, if any, sulfur impurities remain on the catalysts after the hydrogen pretreatment.

Comparisons to Other Model Catalysts. A few recent studies have used solution nanoparticle synthesis methods to prepare supported Au catalysts on high-surface-area oxide supports. Zheng and Stucky showed that titania-supported Au MPCs could be calcined in air at 300 °C for 1 h without causing particle agglomeration.[19] The resulting catalysts were active for ethanol oxidation and showed no residual sulfur in the XPS spectrum. Rolison and co-workers, on the other hand, observed substantial particle growth (2.3 nm prior to treatment, ~6 nm after) for Au MPCs embedded in a titania aerogel after calcination at 425 °C.[20] These catalysts were active for CO oxidation and had residual sulfur present as sulfates. McFarland and co-workers observed a small degree of agglomeration (3.4 nm before treatment, 4.6 nm after) after a 3 h calcination treatment at 300 °C.[21] They also did not observe any sulfur in their XPS spectra, and their catalysts showed activity for propylene partial oxidation, CO oxidation, and propylene hydrogenation.[21,22] Hickey and co-workers calcined ceria-supported MPCs at 250 °C for 5 h and produced active CO oxidation catalysts. They further claimed that their treatment "guarantees the complete removal of the organic monolayer" based on TGA and temperature-programmed oxidation experiments.[23] We also examined thiol removal from MPCs under oxidative, reductive, and inert environments and reported that Au MPCs could be used to prepare active CO oxidation catalysts by treating them at 300 °C under nitrogen for 2 h.[28]

These studies show that it is possible to prepare catalysts from Au MPCs and nanoparticles; however, they generally do not provide comparison of catalytic activity to a standard catalyst prepared by traditional means. A meaningful comparison between traditionally prepared reference catalysts and catalysts derived from solution syntheses is critical to discern how new synthetic methods can be adapted to prepare materials that can be used to study, understand, and improve industrially relevant catalysts. More precise syntheses will also provide insight into the factors that influence the activity of industrial catalysts. Residual sulfur is particularly problematic because sulfides are likely strong poisons for Au catalysts (e.g., Au MPCs with thiol capping ligands are not active catalysts), yet sulfates have been shown to act as promoters for Au-based catalysts.[54] Because of this, kinetic tests to compare catalytic activities are particularly important, as measurements of this nature provide a direct evaluation of surface chemistry and the active site.

Several pretreatment protocols were evaluated in developing the activation protocol used for the Au MPC-based catalysts, including the pretreatments reported by Chou and McFarland[21] and Zheng and Stucky.[19] In our laboratory, neither of these treatments yielded catalysts with significant CO oxidation activity. Further, a yellow product (presumably elemental sulfur) was observed condensing on the exterior of the microreactor tube during the pretreatment immediately before CO oxidation experiments. Some of these differences may be due to the amount of material used in the catalyst activation, with more material requiring greater pretreatment times. However, the differences also indicate that XPS detection limits for the determination of trace amounts of sulfur are not sufficient to guarantee complete sulfur removal, as others have suggested.

(51) Bamwenda, G. R.; Tsubota, S.; Nakamura, T.; Haruta, M. *Catal. Lett.* **1997**, *44*, 83–87.
(52) Comotti, M.; Li, W.-C.; Spliethoff, B.; Schüth, F. *J. Am. Chem. Soc.* **2006**, *128*, 917–924.
(53) Weiher, N.; Beesley, A. M.; Tsapatsaris, N.; Delannoy, L.; Louis, C.; van Bokhoven, J. A.; Schroeder, S. L. M. *J. Am. Chem. Soc.* **2007**, *129*, 2240–2241.
(54) Mohapatra, P.; Moma, J.; Parida, K. M.; Jordaan, W. A.; Scurrell, M. S. *Chem. Commun.* **2007**, 1044–1046.

Materials pretreated with these less forcing activation protocols may still yield active catalysts, but their low CO oxidation activity means that they are not effective models for the most active CO oxidation catalysts. The pretreatment used in the present study (H_2/N_2 at 300 °C for 16 h) yields catalysts that, kinetically, are nearly indistinguishable from the standard WGC catalyst (*vide infra*). This indicates that our reducing treatment removes all of the sulfur from the material (or that any remaining residual sulfur does not substantially block catalysis at the active sites) and that the catalyst is not substantially changed by the reduction treatment. This is an important benchmark for catalysts prepared from Au MPCs, as it allows for future studies examining different preparation methods, support effects, and bimetallic nanoparticles to be compared to catalysts prepared via traditional methods.

Characterization Mechanism and Michaelis−Menten Treatment. Beyond developing a method for preparing new model catalysts from novel synthetic routes, it is important to evaluate new methods for comparing catalytic activity and catalyst parameters. For Au catalysts, where oxygen binding is generally considered to be the critical step for high activity,[2] developing methods for comparing oxygen binding and activation from one catalyst to the next is particularly valuable. To this end, we used a standard surface chemistry reaction mechanism and explored applying a Michaelis−Menten (M-M) algebraic treatment. The goal of this treatment was to evaluate kinetic parameters and provide an additional characterization tool for comparing catalysts.

The original thermodynamic Michaelis−Menten treatment[55] and the steady-state kinetics approach[56] were developed long before protein crystal structures were commonplace, at a time when little was know about the primary structure of proteins and enzymatic active sites were completely uncharacterized. Due to this dearth of structural information, the M-M mechanism was originally developed as a means to extract useful kinetic and mechanistic information from catalytic systems where little is known about the structure of the active site. The generic nature of the M-M approach gives rise to its tremendous utility and has allowed M-M kinetics to be applied to countless enzymatic systems.

Heterogeneous catalysis shares many challenges with enzyme kinetics, particularly the difficulties associated with characterizing active sites. This is especially true for supported gold catalysts, where there has been a substantial debate regarding the nature and location of the CO oxidation active site. Many groups believe that the metal atoms at the interface between the Au catalyst and the oxide support play a role in affecting the active site; however, there is still substantial disagreement over the role of the support, the oxidation state of the metal at the active site, and whether Au can catalyze the reaction without active participation by the support.[2]

Given the similarities between the original application of M-M kinetics and the uncertainties regarding the nature of the active site in heterogeneous catalysts, it may be possible to apply some of the M-M principles to Au-catalyzed CO oxidation and use the extracted parameters as a tool for characterizing catalysts. The general application of M-M treatments to surface reactions has been outlined by Augustine[57] but has not been widely applied to heterogeneous catalysis. We are aware of only one paper describing the use of a M-M treatment to investigate the partial oxidation of 2-propanol over supported Pt catalysts.[58]

Scheme 1. Simplified Mechanism for CO Oxidation over Supported Gold Catalysts

$$\mathrm{Au + CO} \overset{\text{fast}}{\rightleftharpoons} \mathrm{Au\text{-}CO}$$

$$\mathrm{A^* + O_2} \underset{k_{-1}}{\overset{k_1}{\rightleftharpoons}} \mathrm{A^*\text{-}O_2}$$

$$\mathrm{A^*\text{-}O_2 + Au\text{-}CO} \xrightarrow{k_2} \mathrm{A^*\text{-}O + Au + CO_2}$$

$$\mathrm{A^*\text{-}O + Au\text{-}CO} \xrightarrow{\text{fast}} \mathrm{A^* + Au + CO_2}$$

The basic mechanistic steps for CO oxidation (CO adsorption, O_2 adsorption, and surface reactions; see Scheme 1) are standard surface reaction steps that can be interpreted in terms of traditional kinetic models such as the Langmuir−Hinshelwood (L-H) and Eley−Rideal mechanisms.[59] Based on the literature for the particular case of CO oxidation by supported Au catalysts, two reasonable assumptions are warranted: (1) CO binding is fast and strong relative to oxygen binding, thus CO is readily available at or near the active site, and (2) O_2 binding and activation is the key kinetic step in the catalysis. Point (1) is supported by numerous IR spectroscopy studies, including those reported here. Point (2) simply states that CO adsorption on Au, which ought to be largely diffusion-limited, is faster than any surface-mediated reactions that include O═O bond activation. Since CO binds readily to Au catalysts, it is likely that the catalytic activity is primarily associated with O_2 binding and activation.

These assumptions are consistent with previous work, and the mechanism is readily interpreted in terms of the L-H model. The bimolecular L-H model assumes that both reactants of a second-order reaction are bound on the surface, with the reactants diffusing on the surface until they react. Differences in adsorption equilibria are then reflected in differing surface coverages.[60] Inherent in the traditional L-H treatment are the assumptions/simplifications that every surface atom is capable of adsorbing a substrate molecule, that they do so with equal energy, and that there can be only one substrate adsorbed per surface atom.[57,60]

The details of gold-catalyzed CO oxidation allow for the additional consideration of an active site on the catalyst. In particular, the first assumption inherent in the L-H model is not particularly good for CO oxidation over supported Au catalysts. The difficulties associated with laboratory-to-laboratory reproducibility of catalyst activity and in correlating particle size with catalytic activity are good indications that not all surface atoms are equivalent for this reaction.[1,2] More importantly, gold catalysts are extremely susceptible to severe poisoning by even trace (ppm) levels of chloride.[2,61] Indeed, the difference in the amounts of residual chloride from the catalyst synthesis has been suggested as one of the primary

(55) Michaelis, L.; Menten, M. L. *Biochem. Z,* **1913**, *49*, 333–369.
(56) Briggs, G. E.; Haldane, J. B. S. *Biochem. J.* **1925**, *19*, 338–339.
(57) Augustine, R. L. *Heterogeneous Catalysis for the Synthetic Chemist*; Marcel Dekker, Inc.: New York, 1996.
(58) Augustine, R. L.; Doyle, L. K. *J. Catal.* **1993**, *141*, 58–70.
(59) An Ely−Rideal mechanism was also considered. Under our reaction conditions, the Ely−Rideal mechanism (where gas-phase CO attacks surface-bound O_2) is kineticallly indistinguishable from the proposed mechanism. The subtle distinctions are discussed in detail in the Supporting Information.
(60) Somorjai, G. A. *Introduction to Surface Chemistry and Catalysis*; John Wiley & Sons, Inc.: New York, 1994.
(61) Oh, H.-S.; Yang, J. H.; Costello, C. K.; Wang, Y. M.; Bare, S. R.; H, K. H.; Kung, M. C. *J. Catal.* **2002**, *210*, 375–386.

reasons for the different activities measured in different laboratories.[2] The severe poisoning by trace amounts of poisons is an extremely strong indication that there are very few active sites on the catalyst and that the sites are likely to be extremely active for the reaction.

With these parameters in mind, the simplified characterization mechanism shown in Scheme 1 utilizes the idea that particular active sites on the catalyst bind and activate oxygen. Beyond the conclusion that the catalysis occurs at or near a gold surface atom that is capable of binding CO, the mechanism needs no further assumptions regarding the nature or structure of the active site. It merely states that an active site exists where the reaction occurs and that this active site is composed of some subset of the total Au surface atoms (as indicated by chloride poisoning studies).[61] This assumption is widely agreed upon in the literature, although substantial debate remains regarding the nature and structure of the active site (*vide infra*).[1,2] Therefore, in the key kinetic steps of the mechanism, oxygen is bound at an active site (A*) and then reacts with readily available CO to produce CO_2. Subsequent steps to produce a second equivalent of CO_2 and regenerate the active site are considered fast steps after the rate-determining step and are therefore kinetically unobservable.

Control experiments with CO_2 in the feed showed no inhibition of the catalysis, justifying the treatment of CO_2 desorption as irreversible. Treating O═O bond activation as irreversible is consistent with the isotope scrambling studies reported by Calla and Davis.[47] Upon switching the oxygen feed from $^{16}O_2$ to $^{18}O_2$, they observed no production of the mixed isotope species and concluded that either the dissociation of O_2 is irreversible or O_2 does not dissociate. Furthermore, oxygen binding to reduced Au nanoparticles has recently been indirectly detected by X-ray absorption near-edge structure (XANES) and X-ray photoelectron spectroscopies.[53,62–64] The XANES studies suggest that only a fraction of the surface atoms are involved in O_2 binding, consistent with chloride poisoning studies and the characterization mechanism's treatment of readily available CO.

A rate law can be derived from this mechanism using A*-O_2 as a steady-state intermediate and the A* site balance (full derivation supplied as Supporting Information):

$$\nu_{rxn} = \frac{k_1 k_2 [\text{Au-CO}][\text{A*}]_T P_{O_2}}{k_{-1} + k_2[\text{Au-CO}] + k_1 P_{O_2}} \quad (1)$$

A comparable rate law can also be derived in terms of surface coverages and adsorption coefficients using the L-H model, provided that the O_2 activation sites are treated separately from the CO adsorption sites. Two of the advantages of the M-M treatment are that it is more molecular in its language and that it provides ready access to a variety of terms and experiments that have proven to be extremely useful for considering and examining active sites in enzyme catalysis. For instance, three terms can be defined to provide quantitative comparisons for different catalysts and to simplify the expression:

$$k_{ox} = k_2[\text{Au-CO}] \quad (2)$$

$$\nu_{max} = k_{ox}[\text{A*}]_T \quad (3)$$

$$K_I = \frac{k_{-1} + k_{ox}}{k_1} \quad (4)$$

The first term, k_{ox}, is simply an effective rate constant for the second step in the mechanism and is justified by the independence of the reaction rate on CO pressure. The second term, ν_{max}, is analogous to the maximum velocity in M-M kinetics. Since no saturation behavior was observed in the oxygen dependence studies in Figure 7, ν_{max} is simply the extrapolated rate at 100% oxygen (1 atm). As a parameter for characterizing nanoparticle catalysts, ν_{max} contains information regarding the catalytic rate constant and the total number of active sites. The final parameter, K_I, is the ratio of the rate constants associated with the destruction and production of the A*-O_2 intermediate and is analogous to the Michaelis−Menten constant. As with the Michaelis−Menten constant, because K_I describes the rate of intermediate destruction relative to formation, it can therefore be considered a measure of the instability of the O_2-surface intermediate.

The rate law can then be expressed with these new terms,

$$\nu_{rxn} = \frac{k_{ox}[\text{A*}]_T P_{O_2}}{(k_{-1} + k_{ox})/k_1 + P_{O_2}} = \frac{\nu_{max} P_{O_2}}{K_I + P_{O_2}} \quad (5)$$

and rearranged to the double-reciprocal form:

$$\frac{1}{\nu_{rxn}} = \frac{K_I}{\nu_{max}}\left(\frac{1}{P_{O_2}}\right) + \frac{1}{\nu_{max}} \quad (6)$$

Equation 5 is the rate law in the same form as the traditional M-M rate law. The double-inverse form shown in eq 6 has a convenient linear graphical representation that is analogous to the well-known Lineweaver−Burk plots. We want to explicitly point out that the application of this treatment to supported Au catalysts is not an attempt to capture all of the mechanistic detail of the catalyst and the active site. Rather, it is a reductionist approach (as were the early M-M studies) designed to describe only the most basic steps in the catalysis. This approach should be considered a "characterization and evaluation mechanism" in which the primary goal is to develop quantitative analytical tools or metrics that can be used to compare the activity of one heterogeneous catalyst to another. Thus, the essence of this approach is to develop a kinetic description of the catalytic active site.

The oxygen dependence data for both the WGC and Au MPC catalysts can be plotted in this double inverse form to extract ν_{max} and K_I. Figure 9 shows that both catalysts are well described by this treatment at all the temperatures studied. The slope and intercept values from linear regressions of the data plotted in Figure 9 can be found as Supporting Information; extracted values for ν_{max} and K_I are compiled in Table 1.

The treatment of this data allows for a number of conclusions to be drawn. Although the K_I value for the MPC catalyst is slightly larger than for the WGC catalyst, given the standard errors in the determined value of K_I, the differences between the two catalysts probably are not significant. This further supports the other experimental evidence that the MPC method of preparing catalysts results in functional model catalysts. The two catalyst systems have nearly identical particle sizes, indistinguishable rate laws, and essentially the same Arrhenius plots and appear (kinetically, via K_I) to activate oxygen with nearly equivalent efficiency. However, the Au MPC catalyst is roughly 50% more active than the standard WGC catalyst, which

(62) van Bokhoven, J. A.; Louis, C.; Miller, J. T.; Tromp, M.; Safonova, O. V.; Glatzel, P. *Angew. Chem., Int. Ed.* **2006**, *45*, 4651–4654.
(63) Cuenya, B. R.; Baeck, S.-H.; Jaramillo Thomas, F.; McFarland, E. W. *J. Am. Chem. Soc.* **2003**, *125*, 12928–12934.
(64) Bondzie, V. A.; Parker, S. C.; Campbell, C. T. *Catal. Lett.* **1999**, *63*, 143–151.

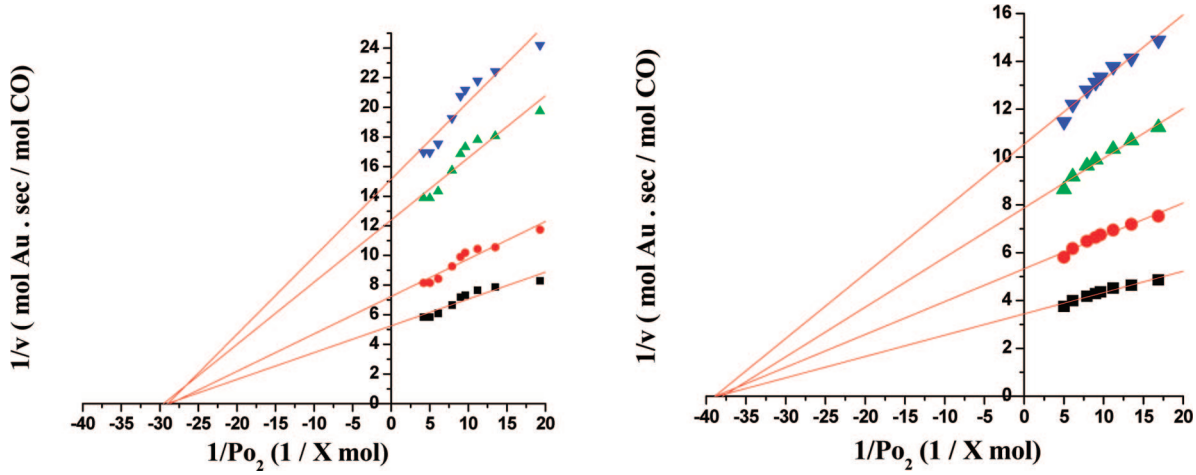

Figure 9. Double-inverse plots of WGC (left) and Au MPC (right) catalysts at (bottom to top) 293, 283, 273, and 268 K.

Table 1. Kinetic Parameters for the Michaelis−Menten Description of WGC and MPC Catalysts

	ν_{max} (min^{-1})		K_I	
temp (K)	WGC	MPC	WGC	MPC
293	11.4 ± 0.6	17.6 ± 0.5	0.035 ± 0.007	0.026 ± 0.003
283	8.3 ± 0.3	11.3 ± 0.3	0.035 ± 0.005	0.026 ± 0.003
273	4.8 ± 0.2	7.7 ± 0.2	0.034 ± 0.006	0.027 ± 0.003
268	4.0 ± 0.2	5.7 ± 0.1	0.035 ± 0.006	0.026 ± 0.003
	average:		**0.035 ± 0.006**	**0.026 ± 0.003**

is shown in Figure 6 and subsequently expressed in the ν_{max} values. Given that K_I contains the rate constant(s) for oxygen activation, it is unlikely that these two catalysts have different intrinsic rate constants that are somehow balanced by antipathetic changes in oxygen binding. Therefore, it is reasonable to conclude that the differences in ν_{max}, which are consistent across the temperature range studied, likely result from differing numbers of active sites. Although the kinetic treatment does not afford an opportunity to determine the absolute number of active sites, the relative values of ν_{max} suggest that the Au MPC catalyst contains approximately 50% more active sites than the WGC catalyst. The reasons for the differences in the number of active sites are unknown at this stage.

For each catalyst, all of the lines in the Figure 9 clearly intersect at the same point (within a reasonable experimental error) on the *x*-axis. This intersection can also be used to estimate K_I (*x*-intercept = $-1/K_I$).[57] The *x*-intercept value is consistent with the value determined from the slope and *y*-intercept, providing strong evidence that the kinetic model is appropriate for describing the data and that the M-M treatment is consistent with the reaction mechanism. In a traditional M-M treatment, this type of plot describes noncompetitive binding, in which the binding of one substrate (or inhibitor) has no effect on the binding of the other,[57] consistent with the proposed mechanism. In one of the early kinetic studies of CO oxidation over gold catalysts, Vannice and co-workers applied a variety of kinetic and mathematical models to describe their kinetic data.[65] Interestingly, they reported the best fitting model to be a Langmuir−Hinshelwood treatment using noncompetitive binding of CO and O_2.[65] They interpreted their data in terms of oxygen adsorption on the support and CO adsorption on the metal; however, more recent isotope exchange experiments by Calla and Davis[47–49] do not support this interpretation. At the same time, their kinetic model of noncompetitive adsorption of CO and O_2 on the catalyst is entirely consistent with both our data and our treatment of the mechanism.

Oxygen Binding by Au Catalysts. Oxygen activation by supported Au catalysts is poorly understood.[2] Although there are several theoretical and UHV surface science studies (*vide infra*), we are aware of no experimental determinations of oxygen binding constants or sticking coefficients for supported Au catalysts. An advantage of the Michaelis−Menten kinetic analysis is that it provides an opportunity to determine O_2 binding constants in the environment where they are most important: under catalytic conditions. The value for K_I can be interpreted in terms of an oxygen binding constant, just as the Michaelis−Menten constant (K_M) is commonly interpreted in enzyme kinetics. Although K_I is strictly defined in terms of the rate constants for the formation and destruction of bound oxygen, it reduces to the inverse of the O_2 binding constant when $k_{ox} \ll k_{-1}$. For these catalysts, this simplification can be justified by the low reaction order for O_2, which suggests that, under the conditions of these experiments, the oxygen binding equilibrium is likely fast and that O═O bond activation (not binding) is rate-determining. The assumption that $k_{ox} \ll k_{-1}$ also makes good chemical sense, as desorption of molecular oxygen, which does not bind strongly to gold, is expected to be fast relative to O═O bond activation. Consequently, this kinetic treatment provides an opportunity to estimate oxygen binding constants during catalysis.

The oxygen binding constant values, which are determined from $1/K_I$, for the Au MPC and WGC catalysts are 38 ± 4 and 29 ± 5, respectively. At 280 K, the middle of the studied temperature range, the average of these equilibrium constants corresponds to an approximate free energy change of −8.5 kJ/

(65) Bollinger, M. A.; Vannice, M. A *Appl. Catal. B, Environ.* **1996**, *8*, 417–443.

mol (or −2.0 kcal/mol, or −0.088 eV). These values show oxygen binding to be very weak,[66] as expected, and they compare favorably with values determined from density functional theory (DFT) calculations and experiments on model UHV systems (*vide infra*). Since K_I can be interpreted in terms of an equilibrium constant, it may be expected to have some temperature dependence; however, no temperature dependence is observed in Table 1. Given the small temperature range studied, it is unlikely that ΔH varies substantially with temperature. The maximum possible variation in the $T\Delta S$ term is 9% from 268 to 293 K; therefore, the total variation in ΔG (and hence K_I) is expected to be substantially smaller. Given that the measurement errors for K_I are on the order of ±10−15%, it is not surprising that any temperature dependence in the O_2 binding constant is masked by the intrinsic errors of the measurement in this limited temperature range.

We have been unable to find comparable measurements of the O_2 binding equilibrium by supported Au catalysts reported in the literature. Two recent XANES studies by van Bokhoven and co-workers provided indirect evidence for oxygen binding to gold nanoparticles supported on alumina and titania.[53,62] Quantifying the interaction was beyond the scope of their study, although they suggested that only a small fraction of the surface atoms were involved in oxygen binding. This is consistent with our results, as two seemingly similar catalysts could reasonably be expected to have substantially different numbers of active sites only if the active sites were just a small fraction of the total surface atoms. This is also consistent with the severe poisoning by trace amounts of chloride reported in the literature.[2] Using relative peak intensities in XPS spectra of Au nanoparticles supported on various polymers, Cuenya et al. concluded that the smallest Au particles contained the largest fraction of bound O_2.[63] Similarly, Bondzie et al. reported that, using model catalysts under UHV conditions, the adsorption of atomic oxygen on small Au particles becomes stronger as the particle size decreases.[64]

At the same time, there are a few quantitative measurments of oxygen binding using model systems in UHV chambers, as well as several recent theoretical studies. There is general consensus in the surface science and computational literature that large, extended planes of Au atoms are incapable of binding and activating oxygen.[67–73] Rather, oxygen binding appears to occur exclusively at edge and corner atoms.[11,64,67,71,74–76] The kinetic O_2 binding constants determined in this work are quite consistent with the few values reported in UHV experiments. Gottfried et al. used several analytical techniques to estimate the binding energy of adsorbed O_2 on a Au(110)-(1×2) surface at less than 3 kcal/mol (0.13 eV).[73] Saliba et al. extracted a similar value for Au(111), estimating the adsorption energy of chemisorbed molecular oxygen to be 3 kcal/mol (0.13 eV).[77]

Several theoretical papers calculate O_2 binding energies that are quite consistent with our kinetic determination (0.088 eV), with values ranging from roughly 0.05 to 0.17 eV. Thomson et al. predicted weakly stable adsorbed states for O_2 on anion clusters of Au_9^- with binding energy of 4 kcal/mol (0.17 eV).[76] Ding et al. calculated a binding energy of 0.09 eV for $Au_6(O_2)$.[78] A major difficulty encountered in using computational techniques is that cluster structures can often be modified upon oxygen adsorption, and small clusters have the capability to exhibit several structural forms (isomers) with comparable energies.[67,79,80] Indeed, Molina and Hammer computed several comparable oxygen binding energies using a Au_{34} cluster (0.03, 0.07, 0.14, 0.17, 0.18, 0.2, and 0.4 eV).[67] The differing adsorption energies corresponded to changes in conformations of the gold particle upon adsorption.

The literature from theoretical and experimental approaches indicates that the catalytic activity of Au nanoparticles is directly related to their ability to bind oxygen (and hence exhibit a zero reaction order in CO). The kinetic determination of O_2 binding by the Au MPC and WGC catalysts agrees well with the values reported in the literature from both theory and surface science measurements. This study, therefore, represents the first experimental evidence showing that the determinations made by the computational and surface science communities can be reasonably extended to working nanoparticle catalysts. The critical structural feature for oxygen binding appears to be the presence of a large number of "rough" atoms (non-flat surfaces), such as edges between facets, corner atoms, kinks, steps, etc. The relative number of these rough atoms is likely influenced by activation procedures, pretreatments, etc., so it is therefore desirable to study oxygen binding by "working" catalysts under real catalytic conditions. The M-M approach provides an additional tool for monitoring heterogeneous catalysts under working conditions, and the good agreement between our experiments and those obtained with other model systems suggests that the general methodology may be applied to other systems in the future.

Comments on the Nature of the Active Site. The nature and location of the active site for CO oxidation by supported gold catalysts remains under debate. There are presently no encompassing conclusions to account for all observations in the literature regarding this matter. Although there are several permutations to the structural models for the active site for CO oxidation, they generally fall into three categories: (I) exclusively reduced Au nanoparticles, possibly with a bilayer gold structure,[46,81] (II) cationic Au or an ensemble of reduced gold clusters with gold cations at the perimeters of such agglomerates,[82,83] and (III) CO activation on Au nanoparticles and oxygen

(66) The entropic contribution to the free energy change during adsorption of a gas molecule to a solid catalyst must be unfavorble; therefore, the slightly exergonic process determined from the equilibrium must also be slightly exothermic.

(67) Molina, L. M.; Hammer, B. *Phys. Rev. B: Condens. Matter Mater. Phys.* **2004**, *69*, 155424/155421–155424/155422.
(68) Hernandez, N. C.; Sanz, J. F.; Rodriguez, J. A. *J. Am. Chem. Soc.* **2006**, *128*, 15600–15601.
(69) *Gmelin Handbook of Inorganic and Organometallic Chemistry*, 8th ed.; Springer-Verlag: Berlin, 1992−94; Vols. B1−B3..
(70) Jansen, M.; Mudring, A. V. In *Gold: Progress in Chemistry, Biochemistry and Technology*; Schmidbaur, H., Ed.; John Wiley & Sons: Chichester, 1999.
(71) Mills, G.; Gordon, M. S.; Metiu, H. *J. Chem. Phys.* **2003**, *118*, 4198–4205.
(72) Deng, X.; Min, B. K.; Guloy, A.; Friend, C. M. *J. Am. Chem. Soc.* **2005**, *127*, 9267–9270.
(73) Gottfried, J. M.; Schmidt, K. J.; Schroeder, S. L. M.; Christmann, K. *Surf. Sci.* **2002**, *511*, 65–82.
(74) Mavrikakis, M.; Stoltze, P.; Norskov, J. K. *Catal. Lett.* **2000**, *64*, 101–106.
(75) Lopez, N.; Norskov, J. K. *J. Am. Chem. Soc.* **2002**, *124*, 11262–11263.
(76) Wells, D. H., Jr.; Delgass, W. N.; Thomson, K. T. *J. Chem. Phys.* **2002**, *117*, 10597–10603.
(77) Saliba, N.; Parker, D. H.; Koel, B. E. *Surf. Sci.* **1998**, *410*, 270–282.
(78) Ding, X.; Li, Z.; Yang, J.; Hou, J. G.; Zhu, Q. *J. Chem. Phys.* **2004**, *120*, 9594–9600.
(79) Hakkinen, H.; Abbet, S.; Sanchez, A.; Heiz, U.; Landman, U. *Angew. Chem., Int. Ed.* **2003**, *42*, 1297–1300.
(80) Prestianni, A.; Martorana, A.; Labat, F.; Ciofini, I.; Adamo, C. *J. Phys. Chem. B* **2006**, *110*, 12240–12248.
(81) Fierro-Gonzalez, J. C.; Gates, B. C. *J. Phys Chem. B.* **2004**, *108*, 16999.
(82) Bond, G. C.; Thomson, D. T. *Gold Bull.* **2000**, *33*, 41.

activation on the titania support. Although this study does not provide direct structural evidence for the active site, the Michaelis−Menten model does provide important kinetic parameters that can be compared to those obtained with relevant computational and UHV models, particularly the O_2 binding constant.

In evaluating the different models, it is first important to clarify that it is possible that more than one type of active site may exist for CO oxidation over supported Au catalysts. Indeed, this might be part of the explanation as to why several notable research groups have reached disparate conclusions regarding the nature of the active site. This is why it is critical to compare the activity of our model MPC catalyst both to that of the standard WGC catalyst and to those of other catalysts reported in the literature.[2] At 273 K, the Haruta,[51] Davis,[47,49] Schüth,[52] and van Bokhoven[53] groups have reported catalyst activities between 0.1 and 0.3 mol $CO \cdot mol^{-1}$ $Au \cdot s^{-1}$; these values are all consistent with the activities reported in this study. Consequently, interpretations regarding oxygen binding and the nature of the active site must be limited to those catalysts that have intrinsic activities, measured at low conversions, in this approximate range. It is possible that different types of active sites dominate catalysts that have substantially different intrinsic activities, or those catalysts where the activity has only been approximated with light-off curves.

Model III above involves oxygen binding by the support and reaction with CO bound to gold nanoparticles. Wu et al. calculated the O_2 binding energy on various TiO_2 surfaces to range from 0.85 to 1.11 eV.[84] These values are substantially larger than the kinetic determination for oxygen binding by our supported gold catalysts. Although this does not definitively rule out oxygen activation on the support, it does suggest that previously undescribed O_2 adsorption sites would need to be present in order to provide adsorption energies comparable to our measurements. These would likely have to be at the nanoparticle−support interface. However, recent transient isotopic exchange experiments reported by Calla and Davis provided no evidence for the support playing a direct role in CO oxidation catalysis.[47–49] A small amount of isotope scrambling between CO_2 and support oxygen was observed, but their careful work showed that this was entirely due to adsorption of CO_2 onto the support after the reaction between CO and O_2. It is difficult to imagine how oxygen adsorbed at the interface of a hydroxylated support would be incapable of exchanging with other oxygen species in such close proximity. Thus, at least for these catalysts, oxygen activation on the Au nanoparticle is most consistent with the kinetic data.

Similarly, our data provide no direct evidence regarding the potential production of cationic Au species associated with the Au nanoparticles. The kinetic description of the active site from the M-M model could be applied to either purely reduced nanoparticles or particles with cationic species near the active site. The catalyst preparation, however, provides greater anecdotal support for reduced active sites than for the participation of oxidized species. The MPC catalyst is prepared by first reducing gold complexes with borohydride, extracting them into a very nonpolar solvent (toluene), and purifying them by repeated precipitation from ethanol. It is therefore unlikely that cationic Au species are present in the deposited MPCs. Further, the nanoparticles were then subjected to a fairly reducing environment of 20% H_2 at 300 °C for 16 h prior to CO oxidation catalysis, which has been shown to have a net reducing environment.[85–87] These catalysts have essentially the same catalytic activity as catalysts prepared via deposition−precipitation with a high-temperature oxidation treatment. Although we cannot rule out the presence of oxidized gold species in the MPC catalyst, we believe that the catalyst preparation means that the active sites are more likely to contain reduced Au species.

Several notable research groups suggest that Au nanoparticles are capable of O_2 activation, regardless of the nature of their interactions with the support.[2] Mavrikakis, Stoltze, and Norskov suggest that the "unusually large" catalytic activity of highly dispersed Au particles may be due to the high step densities on small particles.[74] Similarly, Norskov and others have reported calculations showing that smaller gold particles bind O_2 more strongly than highly coordinated Au atoms[11,78] and that the adsorption of atomic oxygen on small Au particles becomes stronger as the size of the particles decreases.[11] Additionally, Mills and co-workers used DFT to show that the flatness or roughness of the surface very strongly affects oxygen adsorption on both bulk Au and Au clusters.[71] The authors concluded that O_2 does not bind to the flat side of small Au clusters, regardless of the number of electrons in them, and in spite of the fact that the clusters have a "band gap". Goodman's group has also concluded that the unique electronic properties of gold nanoparticles give rise to the high catalytic activity.[43,88,89] Although our study cannot provide structural details regarding the active site, the oxygen binding energy determined with the M-M treatment (−8.5 kJ/mol or −0.088 eV) is most consistent with UHV experiments and quantum mechanical calculations for oxygen adsorption on corner and edge sites of supported Au nanoparticles and thus provides the strongest support for this model.

Conclusions

Monolayer-protected Au clusters were prepared using PAMAM dendrimers as nanoparticle templates and deposited onto titania without significant particle growth. The capping thiol ligands were subsequently removed by an extended treatment in H_2/N_2. The resulting supported Au MPC catalysts were evaluated and compared to a reference catalyst obtained from the World Gold Council. The two catalyst systems were essentially indistinguishable using several characterization techniques (TEM, XPS, and IR spectroscopy of adsorbed CO), and they had essentially identical rate laws and apparent activation energies for CO oxidation catalysis. On the basis of these similarities, the Au MPC catalyst can be considered a functional model gold catalyst: it has the same bulk and catalytic properties as the traditionally prepared WGC catalyst, yet it has a known, reproducible, and modifiable synthetic history. The

(83) Yang, J. H.; Henao, J. P.; Raphulu, M. C.; Wang, J. T.; Caputo, T.; Groszek, A. J.; Kung, M. C.; Scurrell, M. S.; Miller, J. T.; Kung, H. H. *J. Phys. Chem. B* **2005**, *109*, 10319.
(84) Wu, X.; Selloni, A.; Lazzeri, M.; Nayak, S. K. *Phys. Rev. B* **2003**, *68*, 241402.
(85) Yan, W.; Chen, B.; Mahurin, S. M.; Schwartz, V.; Mullins, D. R.; Lupini, A. R.; Pennycook, S. J.; Dai, S.; Overbury, S. H. *J. Phys. Chem. B* **2005**, *109*, 10676–10685.
(86) Schwartz, V.; Mullins, D. R.; Yan, W.; Chen, B.; Dai, S.; Overbury, S. H. *J. Phys. Chem. B* **2004**, *108*, 15782–15790.
(87) Moreau, F.; Bond, G. C.; Taylor, A. O. *J. Catal.* **2005**, *231*, 105–114.
(88) Gross, E.; Asscher, M.; Lundwall, M.; Goodman, D. W. *J. Phys. Chem. C* **2007**, *111*, 16197–16201.
(89) Chen, M.; Cai, Y.; Yan, Z.; Goodman, D. W. *J. Am. Chem. Soc.* **2006**, *128*, 6341–6346.

only significant difference between the two catalyst systems is that, under our experimental conditions, the Au MPC catalyst is approximately 50% more active than the standard WGC catalyst.

A Michaelis−Menten analysis of the catalysts' oxygen dependence allowed for a kinetic characterization of the catalyst. This kinetic analysis allows for a comparison of the number of active sites in each catalyst and indicates that the Au MPC catalyst contains roughly 50% more active sites than the traditionally prepared WGC material. In addition, the M-M treatment allowed for a determination of the oxygen binding constant under catalytic conditions. To the best of our knowledge, no other direct experimental measurements of oxygen binding by supported Au catalysts have been reported. Several reports describe oxygen binding in UHV model systems and in computational studies, and these values are in good agreement with the kinetic determinations reported here. The binding constants determined in this work are most consistent with values obtained by UHV experiments and quantum theory that suggest O_2 binding occurs at edge or corner sites on gold nanoparticles.

Acknowledgment. The authors gratefully acknowledge the Robert A. Welch Foundation (Grant Nos. W-1552 and F-1529) and the U.S. National Science Foundation (Grant No. CHE-0449549) for financial support of our work.

Supporting Information Available: Schematic diagram of CO oxidation reactor system, UV−visible spectra, XPS survey scans, CO reaction orders, kinetic data, rate law derivation, and comparison of L-H, E-R, and M-M models. This material is available free of charge via the Internet at http://pubs.acs.org.

JA801279A

Kinetic Characterization of Highly Active Supported Gold Catalysts from Monolayer Protected Clusters: An Experimental Michaelis-Menton Approach for Determining the Oxygen Binding Constant During CO Oxidation Catalysis

Cormac G. Long,[A] John D. Gilbertson,[A] Ganesh Vijayaraghavan,[B] Keith J. Stevenson,[B] Christopher J. Pursell, and Bert D. Chandler[*,A]

[A]Department of Chemistry, Trinity University, San Antonio, TX 78212-7200, and

[B]Department of Chemistry, University of Texas at Austin, 1 University Station A5300, Austin, TX 78712-0165

[*]To Whom Correspondence Should be Addressed:

(210) 999-7557 phone; (210) 999-7569 fax; Bert.chandler@trinity.edu

---

Table of Contents

Figure S1. Schematic diagram of CO Oxidation Reactor system.

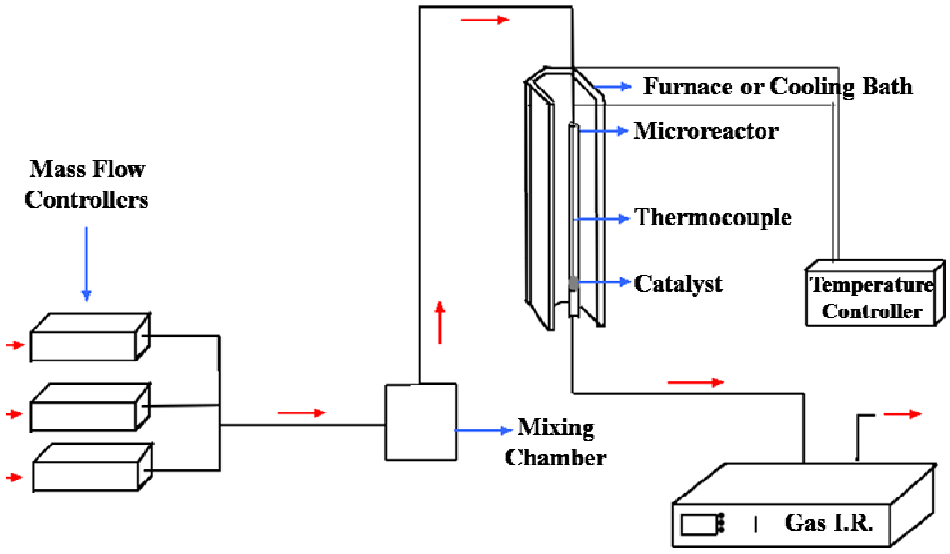

Figure S2. Solution UV-vis spectra of $G_5OH(Au_{147})$ DENs (bottom, blue) and $C_{10}S(Au)$ MPCs (top, red).

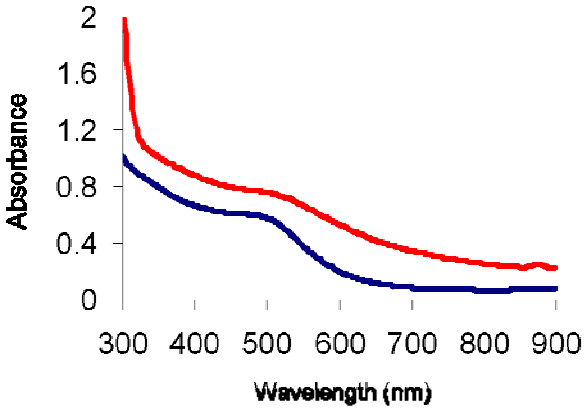

Figure S3. XPS survey scan of MPC catalyst

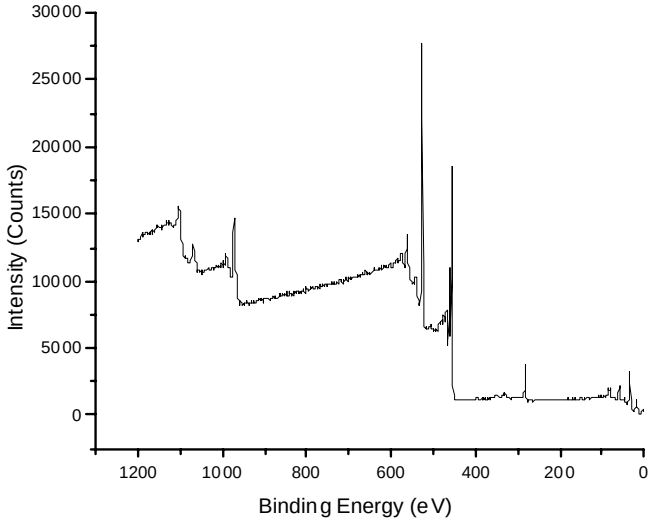

Figure S4. XPS survey scan of WGC catalyst

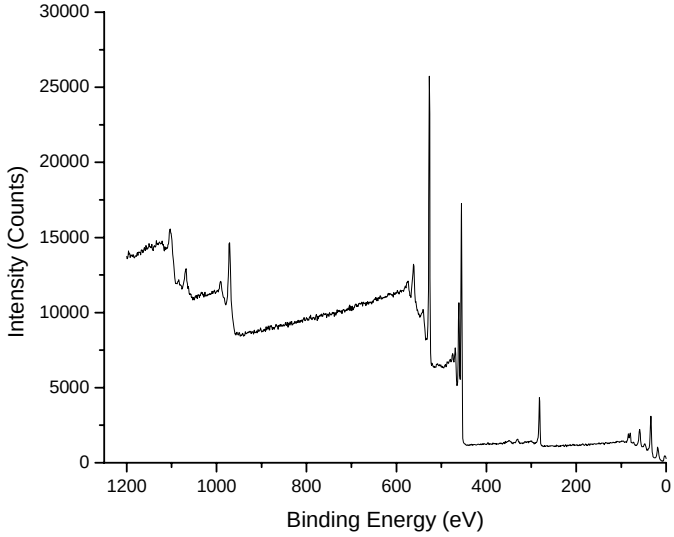

Figure S5. WGC catalyst activity with and without reduction treatment compared to MPC catalyst. Reaction conditions: 1% CO, 20% O_2.

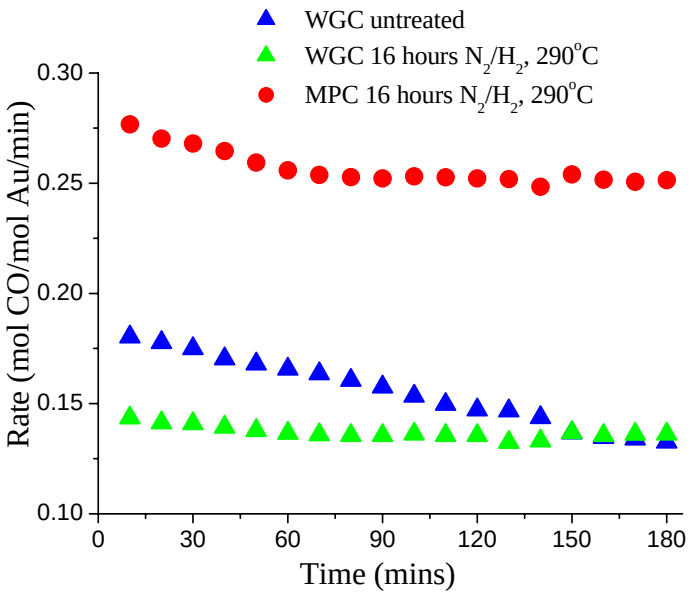

Figure S6. CO reaction order for MPC and WGC catalysts at 20% O_2.

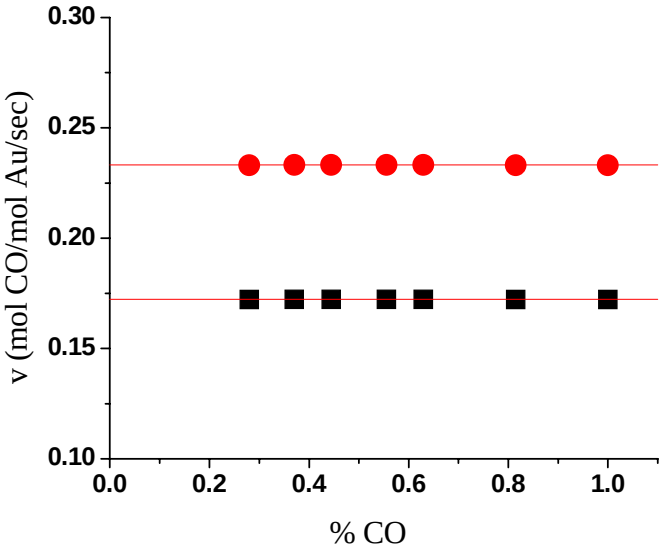

Table S1. Oxygen Reaction Orders.

Temperature (K)	O_2 Reaction Order	
	WGC	MPC
293	0.18 ± 0.01	0.19 ± 0.01
283	0.20 ± 0.02	0.20 ± 0.01
273	0.19 ± 0.02	0.20 ± 0.01
268	0.20 ± 0.01	0.19 ±0.01

Table S2. WGC catalyst kinetic data

	Rate				For 1/ν vs 1/P_{O2} plots 1/ν				
PO2/Ptot	**293 K**	**283 K**	**273 K**	**263 K**	Ptot/PO2	**293 K**	**283 K**	**273 K**	**263 K**
0.23704	0.171	0.123	0.072	0.059	4.2	5.85	8.15	13.86	16.97
0.2	0.171	0.123	0.072	0.059	5.0	5.85	8.15	13.86	16.97
0.16296	0.164	0.119	0.07	0.057	6.1	6.09	8.42	14.33	17.54
0.12593	0.15	0.108	0.064	0.052	7.9	6.65	9.26	15.74	19.27
0.11111	0.139	0.101	0.059	0.048	9.0	7.19	9.91	16.85	20.76
0.1037	0.137	0.098	0.058	0.047	9.6	7.33	10.19	17.31	21.19
0.08889	0.131	0.096	0.056	0.046	11.2	7.66	10.44	17.80	21.79
0.07407	0.127	0.095	0.055	0.045	13.5	7.88	10.56	18.05	22.44
0.05185	0.121	0.085	0.051	0.041	19.3	8.29	11.74	19.74	24.20
					slope	0.181	0.253	0.421	0.524
					error	0.025	0.028	0.05	0.063
					% error	13.9%	11.1%	11.9%	12.1%
					intercept	5.244	7.229	12.37	15.12
					error	0.265	0.296	0.53	0.666
					% error	5.0%	4.1%	4.3%	4.4%
					vmax	0.191	0.138	0.081	0.066 sec
						11.44	8.3	4.849	3.968 min
					error	0.577	0.34	0.208	0.175
					KI	0.035	0.035	0.034	0.035
					error	0.007	0.005	0.006	0.006
					% error	18.9%	15.2%	16.2%	16.5%
					Keq	29	29	29	29
					error	5	4	5	5

Table S3. MPC catalyst kinetic data

	Rate				For 1/ν vs 1/P_{O2} plots 1/ν				
PO2/Ptot	**293 K**	**283 K**	**273 K**	**263 K**	Ptot/PO2	**293 K**	**283 K**	**273 K**	**263 K**
0.200	0.266	0.172	0.116	0.087	5.0	3.75	5.81	8.64	11.48
0.163	0.251	0.162	0.109	0.082	6.1	3.99	6.17	9.18	12.20
0.126	0.239	0.154	0.104	0.078	7.9	4.18	6.48	9.63	12.80
0.111	0.233	0.151	0.101	0.076	9.0	4.29	6.64	9.88	13.12
0.104	0.229	0.148		0.075	9.6	4.36	6.75		13.35
0.089	0.221	0.144	0.097	0.073	11.2	4.52	6.94	10.33	13.78
0.074	0.215	0.139	0.094	0.071	13.5	4.64	7.18	10.68	14.13
0.059	0.206	0.133	0.089	0.067	16.9	4.86	7.53	11.24	14.89
					slope	0.089	0.138	0.209	0.272
					error	0.008	0.011	0.016	0.023
					% error	8.6%	8.2%	7.7%	8.3%
					intercept	3.438	5.322	7.865	10.52
					error	0.081	0.119	0.172	0.24
					% error	2.4%	2.2%	2.2%	2.3%
					vmax	0.291	0.188	0.127	0.095 sec
						17.45	11.27	7.629	5.705 min
					error	0.411	0.252	0.166	0.13
					KI	0.026	0.026	0.027	0.026
					error	0.003	0.003	0.003	0.003
					% error	10.9%	10.4%	9.9%	10.6%
					Keq	38	39	38	39
					error	4	4	4	4

Rate Law Derivation

$$Au + CO \overset{fast}{\rightleftharpoons} Au\text{-}CO$$

$$A^* + O_2 \underset{k_{-1}}{\overset{k_1}{\rightleftharpoons}} A^*\text{-}O_2$$

$$A^*\text{-}O_2 + Au\text{-}CO \xrightarrow{k_2} A^*\text{-}O + Au + CO_2$$

$$A^*\text{-}O + Au\text{-}CO \xrightarrow{fast} A^* + Au + CO_2$$

The reaction rate is defined in terms of the second step:

$$\nu_{rxn} = k_2[Au-CO][A^*-O_2]$$

The active site balance is:

$$[A^*]_T = [A^*] + [A^*-O_2]$$

Using A*-O_2 as the steady state intermediate, the steady state approximation yields:

$$\frac{d[A^*-O_2]}{dt} = k_1 P_{O_2}[A^*] - k_{-1}[A^*-O_2] - k_2[Au-CO][A^*-O_2] = 0$$

Solving for [A*] yields:

$$[A^*] = \frac{\left(k_{-1} + k_2[Au-CO]\right)[A^*-O_2]}{k_1 P_{O_2}}$$

Substituting into the active site balance yields:

$$[A^*]_T = \left(\frac{\left(k_{-1} + k_2[Au-CO]\right)}{k_1 P_{O_2}} + 1\right)[A^*-O_2]$$

Solving for [A*-O_2] yields:

$$[A^*-O_2] = \frac{k_1 P_{O_2}[A^*]_T}{k_{-1} + k_2[Au-CO] + k_1 P_{O_2}}$$

Substituting into the rate expression yields:

$$\nu_{rxn} = \frac{k_1 k_2[Au-CO] P_{O_2}[A^*]_T}{k_{-1} + k_2[Au-CO] + k_1 P_{O_2}}$$

Three terms can be defined to provide quantitative comparisons for different catalysts and simplify the expression.

$$k_{ox} = k_2[Au-CO] \qquad \nu_{\max} = k_{ox}[A^*]_T \qquad K_I = \frac{k_{-1}+k_{ox}}{k_1}$$

The rate law can then be expressed in terms of k_{ox}:

$$\nu_{rxn} = \frac{k_1 k_{ox} P_{O_2}[A^*]_T}{k_{-1}+k_{ox}+k_1 P_{O_2}}$$

Rearranging the rate law and expressing in terms of ν_{max} and K_I yields a simplified rate law:

$$\nu_{rxn} = \frac{k_{ox}[A^*]_T P_{O_2}}{\frac{k_{-1}+k_{ox}}{k_1}+P_{O_2}} = \frac{\nu_{\max} P_{O_2}}{K_I + P_{O_2}}$$

The simplified rate law can then be rearranged to the double reciprocal form:

$$\frac{1}{\nu_{rxn}} = \frac{K_I}{\nu_{\max}}\left(\frac{1}{P_{O_2}}\right)+\frac{1}{\nu_{\max}}$$

Comparing Langmuir-Hinshelwood, Ely-Rideal, and Michelis-Menten Treatments

The key difference between the L-H and E-R models and our application of the M-M model is the treatment of the active site. Whereas the L-H and E-R models treat all surface atoms equivalently, our treatment assumes that there is some arrangement of atoms that constitutes the active site for CO oxidation, and that the active site includes only a subset of the total surface Au atoms. This treatment is justified by a number of previous experimental observations and is consistent with a number of models available in the literature (vida infra). The kinetic M-M model does not involve a direct assumption regarding the nature of the active site; it merely asserts that there are particular sites on the catalyst surface capable of binding and activating oxygen. Additionally, the M-M treatment provides ready access to approaches from

enzyme catalysis that allow for the consideration and examination of an active site. The common use of double inverse plots is a simple means of determining valuable kinetic parameters, such as the reactant binding energies at the active site. It also provides for a means of evaluating a relative number of active sites and changes to the active site (through the maximum turnover frequency and inhibition experiments), which has not been the common practice using more traditional kinetic models for surface chemistry.

Beyond the differences in the treatment of the active site, there are some more subtle similarities and differences between our application of M-M kinetics and the Eley-Rideal (E-R) model. Two possibilities must be considered in evaluating the E-R model: (1) that gas phase O_2 reacts with CO bound to the surface and (2) that gas phase CO reacts with O_2 bound to the surface. The first case might be plausible because CO adsorption on Au is readily observed in IR spectra. However, given that the O=O double bond must be broken in the reaction, it is unlikely that this will occur without some degree of activation by the metal. Indeed, studies with bimetallic Au-Pt catalysts prepared from different precursors have shown that CO can bind on Au sites, yet the bimetallic catalysts do not necessarily show the high CO oxidation activity associated with monometallic Au catalysts.[1-3] Thus, Amiridis and coworkers concluded that the presence of Au based CO binding sites is necessary but not sufficient for high CO oxidation activity.[2]

The possibility that O_2 is activated on the metal and subsequently attacked by CO must also be considered in light of the surface CO coverage and zero order CO kinetics. It is important to highlight that the zero reaction order in CO means only that the reaction is kinetically saturated with CO; it does not necessarily imply that the Au surface is saturated in CO. Pressure studies of CO adsorption on supported gold catalysts show that CO continues to

adsorb on the gold sites as pressure increases from 7 to 150 torr.[4] This indicates that, although CO is bound more strongly on Au than O_2, it is unlikely that the surface of the gold nanoparticles is saturated with CO (i.e. every surface Au atom is bound to a CO molecule) under typical reaction conditions (2-10 torr CO and 5-150 torr O_2). Thus, the reaction can be *kinetically* saturated to reach a 0 order in CO without having the surface physically saturated in CO. This is an important distinction, because it means that oxygen adsorption sites (the active sites in both this E-R and the M-M models) are available.

In both of these models, reaction between adsorbed O_2 and either gas phase (E-R model) or adsorbed (our M-M treatment) CO is the next step. Under the reaction conditions available for our study, these two cases are kinetically indistinguishable when CO adsorption on Au is fast, which is likely. Thus, once the treatment of the active site is considered, our treatment with the M-M model is entirely consistent with the E-R model under the kinetic regime of this study – the only difference between the two models is whether attack on the surface-bound O_2 comes from gas phase or adsorbed CO. Given that CO adsorption and exchange with the surface is likely to be fast, this subtle distinction will be extremely difficult to unequivocally determine. Because the kinetic treatment employed here was based on the zero reaction order for CO, the source of CO (gas phase or adsorbed) affects only the terminology used to describe the second step of our model, not the kinetics of the process. This actually highlights the utility of primarily considering the active sites in the M-M treatment, and validates the importance of focusing on O_2 binding and activation as the key step in the reaction mechanism.

(1) Auten, B.; Lang, H.; Chandler, B. D. *Applied Catalysis B: Environmental* **2008**, in press.
(2) Ortiz-Soto, L. B.; Alexeev, O. S.; Amiridis, M. D. *Langmuir* **2006**, *22*, 3112-3117.
(3) Lang, H.; Maldonado, S.; Stevenson, K. J.; Chandler, B. D. *J. Am. Chem. Soc.* **2004**, *126*, 12949-12956.

(4) Derrouiche, S.; Gravejat, P.; Bianchi, D. *J. Am. Chem. Soc.* **2004**, *126*, 13010-13015.